Science Advances
AAAS

Supplementary Materials for

Glycogen synthase kinase 3 drives thymocyte egress by suppressing β-catenin activation of Akt

Chenfeng Liu, Lei Ma, Yuxuan Wang, Jiayi Zhao, Pengda Chen, Xian Chen, Yingxin Wang, Yanyan Hu, Yun Liu, Xian Jia, Zhanghua Yang, Xingzhi Yin, Jianfeng Wu, Suqin Wu, Haiping Zheng, Xiaohong Ma, Xiufeng Sun, Ying He, Lianghua Lin, Yubing Fu, Kunyu Liao, Xiaojuan Zhou, Shan Jiang, Guofeng Fu, Jian Tang, Wei Han, Xiao Lei Chen, Wenzhu Fan, Yazhen Hong, Jiahuai Han, Xiangyang Huang, Bo-An Li, Nengming Xiao, Changchun Xiao*, Guo Fu*, Wen-Hsien Liu*

*Corresponding author. Email: whliu@xmu.edu.cn (W.-H.L.); guofu@xmu.edu.cn (G.F.); cxiao@xmu.edu.cn (C.X.)

Published 8 October 2021, *Sci. Adv.* **7**, eabg6262 (2021)
DOI: 10.1126/sciadv.abg6262

This PDF file includes:

Fig. S1

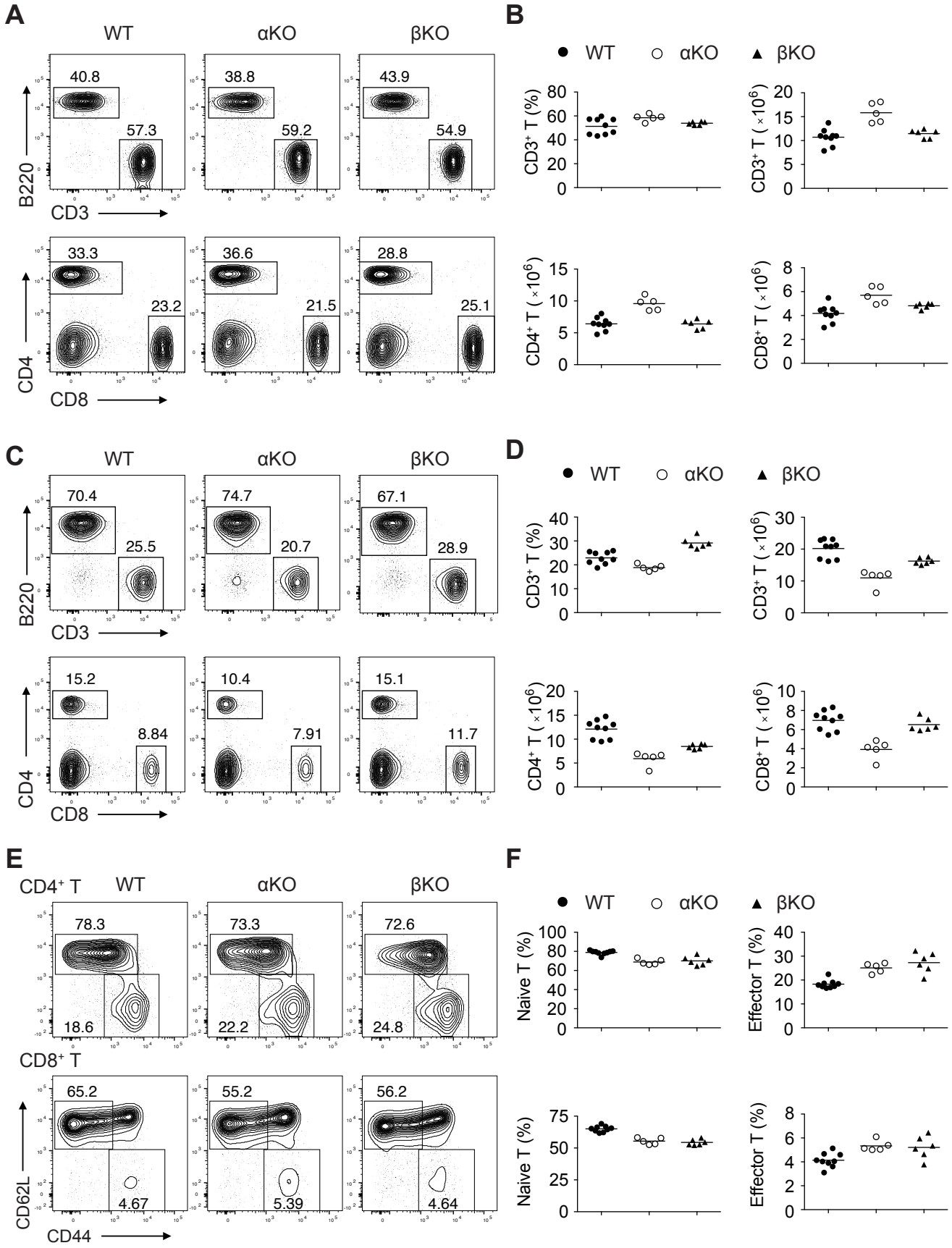
A
WT
αKO
βKO
40.8
57.3
38.8
59.2
43.9
54.9
B220
CD3
33.3
23.2
36.6
21.5
28.8
25.1
CD4
CD8
B
WT
αKO
βKO
CD3⁺ T (%)
CD3⁺ T (×10⁶)
CD4⁺ T (×10⁶)
CD8⁺ T (×10⁶)
C
WT
αKO
βKO
70.4
25.5
74.7
20.7
67.1
28.9
B220
CD3
15.2
8.84
10.4
7.91
15.1
11.7
CD4
CD8
D
WT
αKO
βKO
CD3⁺ T (%)
CD3⁺ T (×10⁶)
CD4⁺ T (×10⁶)
CD8⁺ T (×10⁶)
E
CD4⁺ T
WT
αKO
βKO
78.3
18.6
73.3
22.2
72.6
24.8
CD8⁺ T
65.2
4.67
55.2
5.39
56.2
4.64
CD62L
CD44
F
WT
αKO
βKO
Naive T (%)
Effector T (%)
Naive T (%)
Effector T (%)

Fig. S1. Normal peripheral T cell compartments in *Gsk3α*$^{-/-}$ and *Gsk3b*$^{-/-}$ mice

(A-D) Flow cytometry analysis of CD3$^+$ T and B220$^+$ B cells (upper), CD4$^+$ and CD8$^+$ T cells (lower) in the lymph nodes (A and B) and spleen (C and D) of 4-6 week-old WT, *Gsk3α*$^{-/-}$(αKO) and *Gsk3b*$^{-/-}$(βKO) mice. (A and C) Representative FACS plots. (B and D) Summary of the percentage and number of CD3$^+$TCRβ$^+$ (upper) and CD4$^+$ and CD8$^+$ T cells (lower) in the lymph nodes (B) and spleen (D) (n≥5 per group). (E and F) Flow cytometry analysis of naive (CD62L$^+$CD44$^-$) and activated (CD62L$^-$CD44$^+$) T cells among CD4$^+$ (upper) and CD8$^+$ T cells (lower) in the spleen of WT, αKO and βKO mice. (E) Representative FACS plots. (F) Summary of the percentages of naive and activated T cells. Each symbol represents an individual mouse; small horizontal lines indicate the mean (± s.e.m.). Data are representative of at least two independent experiments.

Fig. S2

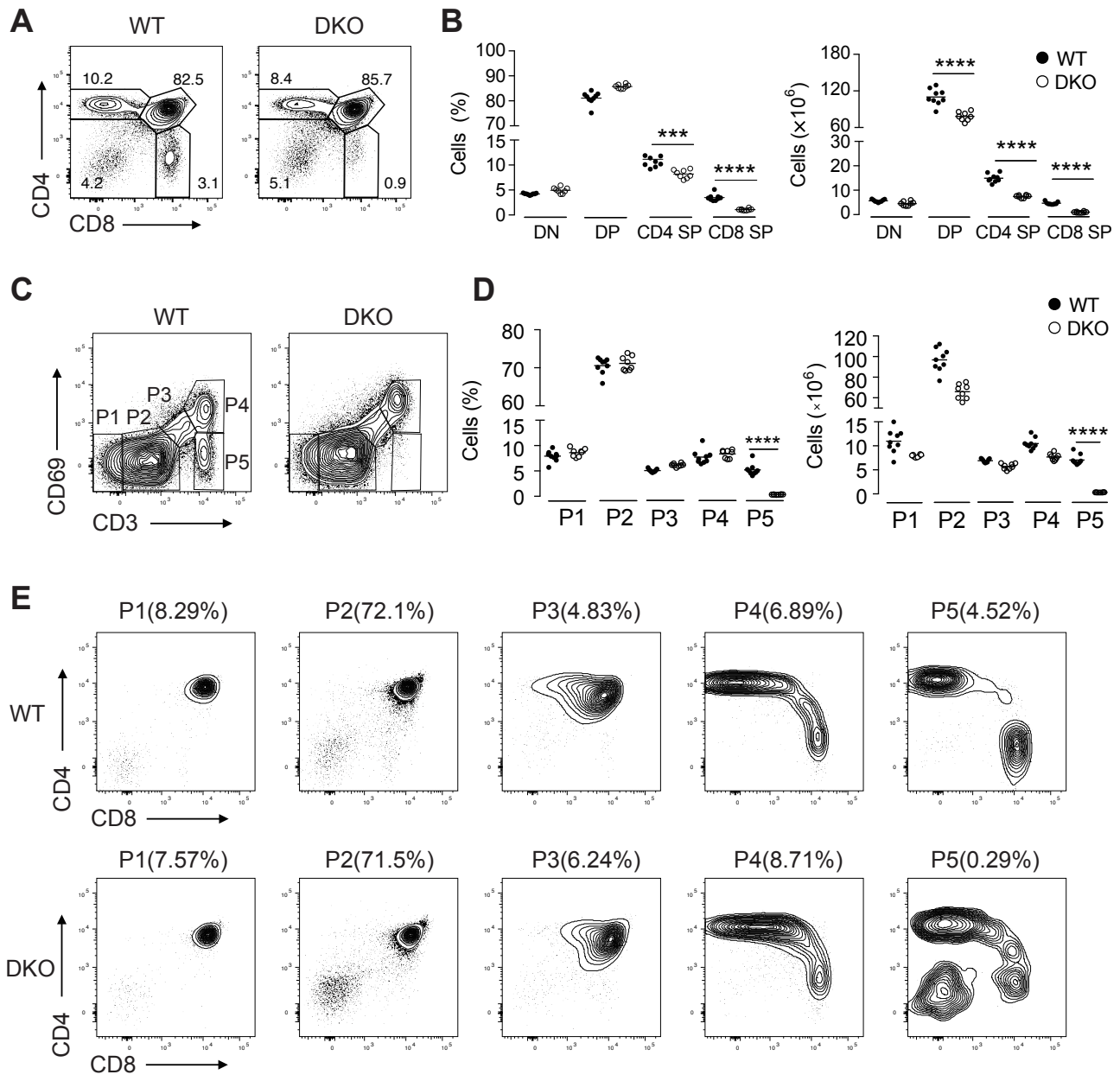
A
WT
DKO
10.2
82.5
4.2
3.1
8.4
85.7
5.1
0.9
CD4
CD8
B
Cells (%)
Cells (×10^6)
WT
DKO
****
***
DN
DP
CD4 SP
CD8 SP
C
CD69
CD3
P1 P2
P3
P4
P5
D
P1
P2
P3
P4
P5
E
P1(8.29%)
P2(72.1%)
P3(4.83%)
P4(6.89%)
P5(4.52%)
P1(7.57%)
P2(71.5%)
P3(6.24%)
P4(8.71%)
P5(0.29%)

Fig. S2. Thymocyte development in *Gsk3a*$^{-/-}$*b*$^{-/-}$ mice

(A) Flow cytometry analysis of thymocytes from 4-6 week-old WT and DKO mice. (B) Percentage and number of DN, DP, $CD4^+$ and $CD8^+$ SP populations from (A) (n≥8 per group). (C-E) Thymocytes from WT and DKO mice were divided into five subpopulations (P1-P5) based on CD3 and CD69 expression (C and D). These subpopulations were further examined for CD4 and CD8 expression (E). (C and E) Representative FACS plots. (D) Summary of the percentage and number of P1-P5 subpopulations in WT and DKO mice (n≥4 per group). Note that DKO mice lack the P5 subpopulation, which are mature SP thymocytes ready for emigration from the thymus. Each symbol represents an individual mouse. Small horizontal lines indicate the mean (± s.e.m.). ***, $P < 0.001$; ****, $P < 0.0001$. Data are representative of at least three independent experiments.

Fig. S3

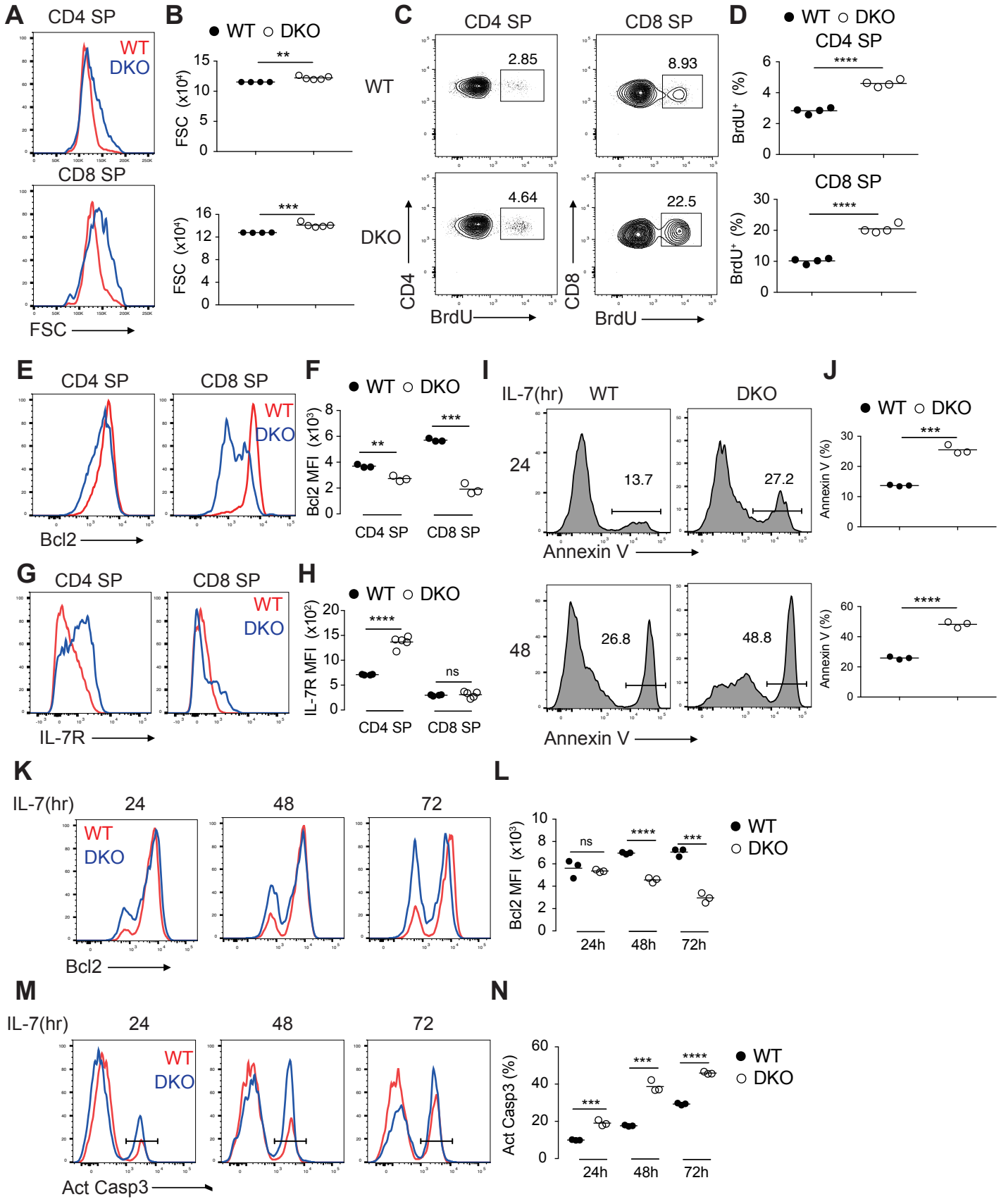
A
CD4 SP
WT
DKO
CD8 SP
FSC
B
WT DKO
FSC (x10⁴)
**
***
C
CD4 SP
CD8 SP
WT
DKO
2.85
8.93
4.64
22.5
CD4
CD8
BrdU
D
WT DKO
CD4 SP
CD8 SP
BrdU⁺ (%)
****
E
CD4 SP
CD8 SP
WT
DKO
Bcl2
F
WT DKO
Bcl2 MFI (x10³)
CD4 SP
CD8 SP
G
CD4 SP
CD8 SP
WT
DKO
IL-7R
H
WT DKO
IL-7R MFI (x10²)
ns
I
IL-7(hr)
WT
DKO
24
48
13.7
27.2
26.8
48.8
Annexin V
J
WT DKO
Annexin V (%)
K
IL-7(hr)
24
48
72
WT
DKO
Bcl2
L
Bcl2 MFI (x10³)
ns
24h
48h
72h
WT
DKO
M
IL-7(hr)
24
48
72
WT
DKO
Act Casp3
N
Act Casp3 (%)
24h
48h
72h
WT
DKO

Fig. S3. GSK3 promotes survival of SP thymocytes

(A-D) Flow cytometry analysis of size and proliferation of CD4 and CD8 SP thymocytes from 4-6 week-old WT (red) and DKO (blue) mice at 16 hours after BrdU injection. FSC, forward scatter. n=4 per group. (B) Summary of FSC. (D) Summary of the percentage of $BrdU^+$ cells among CD4 (upper) and CD8 SP thymocytes (lower). (E-H) Flow cytometry analysis of DP, CD4 and CD8 SP thymocytes from WT (red) and DKO (blue) mice for intracellular Bcl2 (E) and surface IL-7R (G) expression. MFI of Bcl2 (F) and IL-7R (H) expression on CD4 and CD8 SP thymocytes. (I and J) Annexin V staining of CD4 SP thymocytes stimulated with 1 ng/ml IL-7 for 24 and 48 hours. (J) Summary of the percentage of Annexin V^+ cells. (K-N) Intracellular staining of Bcl2 (K and L) and active caspase 3 (M and N) in CD4 SP thymocytes stimulated with 1 ng/ml IL-7 for 24, 48, and 72 hours. (L) MFI of Bcl2. (N) Summary of the percentage of active caspase 3^+ cells. Each symbol represents an individual mouse. Small horizontal lines indicate the mean (± s.e.m.). **, $P < 0.01$; ***, $P < 0.001$; ****, $P < 0.0001$. Data are representative of at least two independent experiments.

Fig. S4

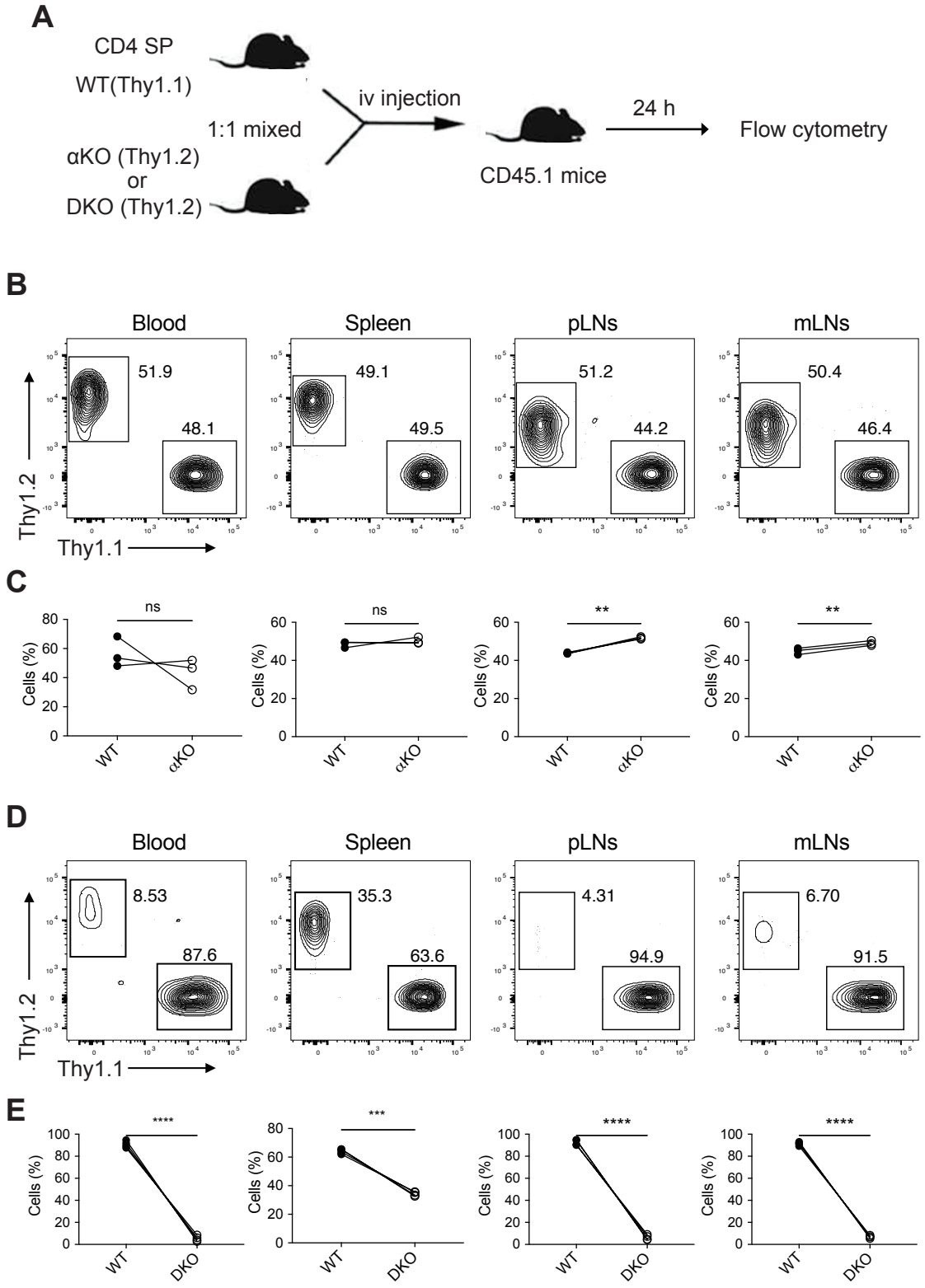
A
CD4 SP
WT(Thy1.1)
1:1 mixed
αKO (Thy1.2)
or
DKO (Thy1.2)
iv injection
CD45.1 mice
24 h
Flow cytometry
B
Blood
Spleen
pLNs
mLNs
51.9
48.1
49.1
49.5
51.2
44.2
50.4
46.4
Thy1.2
Thy1.1
C
ns
ns
**
**
Cells (%)
WT
αKO
D
Blood
Spleen
pLNs
mLNs
8.53
87.6
35.3
63.6
4.31
94.9
6.70
91.5
Thy1.2
Thy1.1
E
****
***
****
****
Cells (%)
WT
DKO

Fig. S4. Homing defect of *Gsk3*-deficient CD4 SP thymocytes

(A) Experimental outline. CD4 SP thymocytes from WT (Thy1.1$^+$) and αKO (Thy1.2$^+$) or DKO (Thy1.2$^+$) mice (all CD45.2$^+$) were mixed in a 1:1 ratio, adoptively transferred to CD45.1$^+$ recipient mice, followed by flow cytometry analysis of blood, spleen, peripheral and mesenteric lymph nodes (pLNs and mLNs) at 24 hours after transfer. (B-E) Flow cytometry analysis of CD45.2$^+$Thy1.1$^+$ and CD45.2$^+$Thy1.2$^+$ cells in blood, spleen, pLNs and mLNs of CD45.1$^+$ recipient mice. (B and D) Representative FACS plots. (C and E) Summary of the percentage and numbers of CD45.2$^+$Thy1.1$^+$ and CD45.2$^+$Thy1.2$^+$ cells. Each symbol represents an individual mouse. Small horizontal lines indicate the mean (± s.e.m.). **, P <0.01; ***, P < 0.001; ****, P < 0.0001. Data are representative of two independent experiments.

Fig. S5

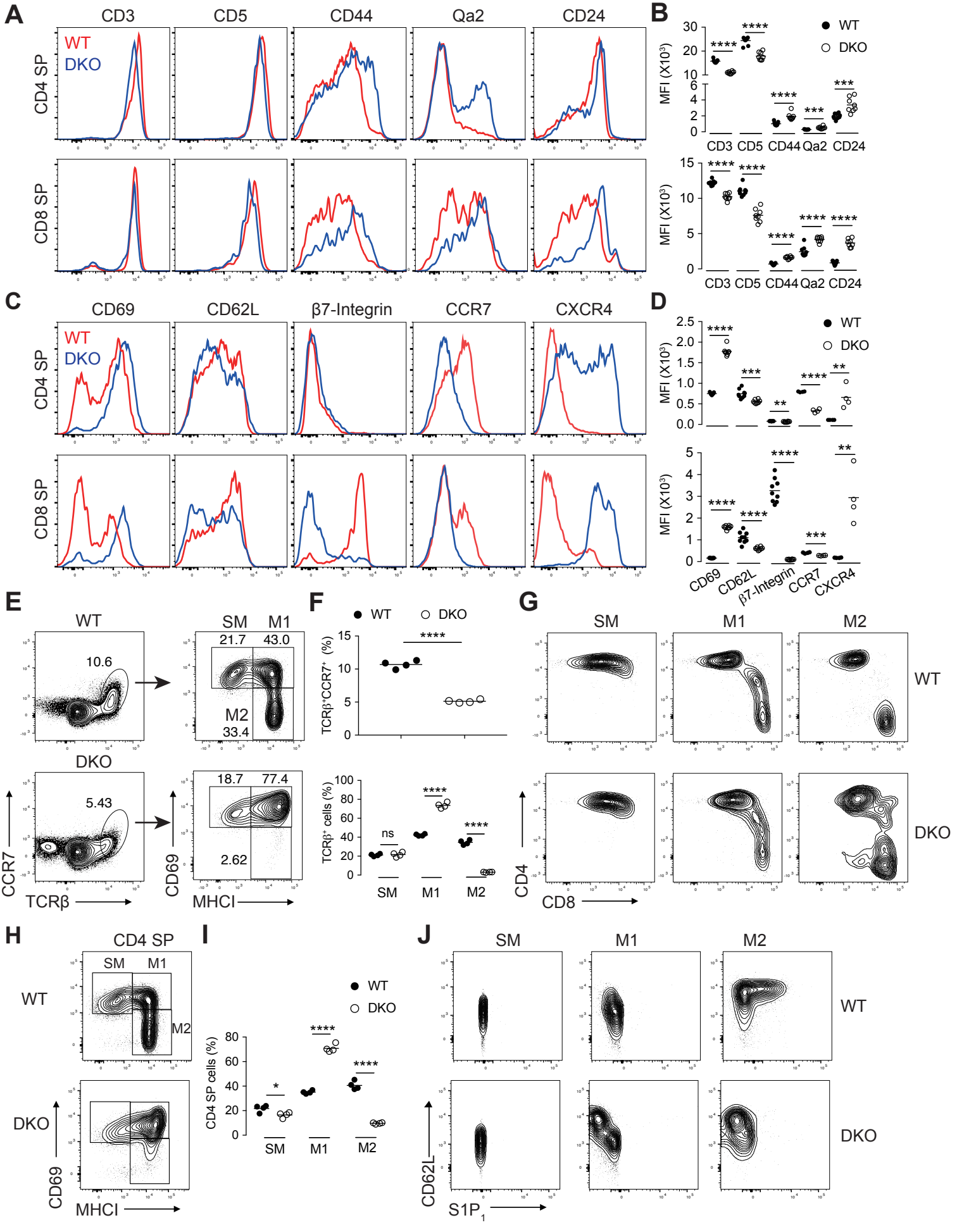
A
CD3
CD5
CD44
Qa2
CD24
WT
DKO
CD4 SP
CD8 SP
B
WT
DKO
MFI (X10³)
CD3 CD5 CD44 Qa2 CD24
C
CD69
CD62L
β7-Integrin
CCR7
CXCR4
D
CD69 CD62L β7-Integrin CCR7 CXCR4
E
WT
DKO
SM M1
M2
10.6
21.7
43.0
33.4
5.43
18.7
77.4
2.62
CCR7
TCRβ
CD69
MHCI
F
TCRβ⁺CCR7⁺ (%)
TCRβ⁺ cells (%)
ns
SM M1 M2
G
SM M1 M2
WT
DKO
CD4
CD8
H
CD4 SP
SM M1
M2
WT
DKO
CD69
MHCI
I
CD4 SP cells (%)
SM M1 M2
J
SM M1 M2
WT
DKO
CD62L
S1P1

Fig. S5. GSK3 controls expression of molecules critical for thymocyte trafficking

(A-D) Flow cytometry analysis of maturation (A and B) and trafficking molecules (C and D) on CD4 (upper) and CD8 (lower) SP thymocytes from 4-6 week-old WT and DKO mice. MFI of indicated maturation (B) and trafficking molecules (D). (E) Flow cytometry analysis of CCR7 and TCRβ expression on thymocytes from WT and DKO mice. Post-positive selection thymocytes ($CCR7^{+}TCR\beta^{+}$) were separated into three subpopulations (SM, M1 and M2) based on CD69 and MHC I expression (E), followed by analysis of CD4 and CD8 expression (G). (F) Summary of the percentage of $CCR7^{+}TCR\beta^{+}$ (upper) and $TCR\beta^{+}$ cells gated on SM, M1 and M2 subpopulations (lower). (H) Flow cytometry analysis of CD69 and MHC I expression on CD4 SP thymocytes from WT and DKO mice. (I) Summary of the percentage of CD4 SP cells gated on SM, M1 and M2 subpopulations. (J) Flow cytometry analysis of CD62L and $S1P_1$ expression on SM, M1 and M2 subpopulations of CD4 SP thymocytes from WT and DKO mice ($n \geq 4$ per group). Each symbol represents an individual mouse. Small horizontal lines indicate the mean (± s.e.m.). *, $P < 0.1$; **, $P < 0.01$; ***, $P < 0.001$; ****, $P < 0.0001$. Data are representative of three (A-D) and two (E-J) independent experiments.

Fig. S6

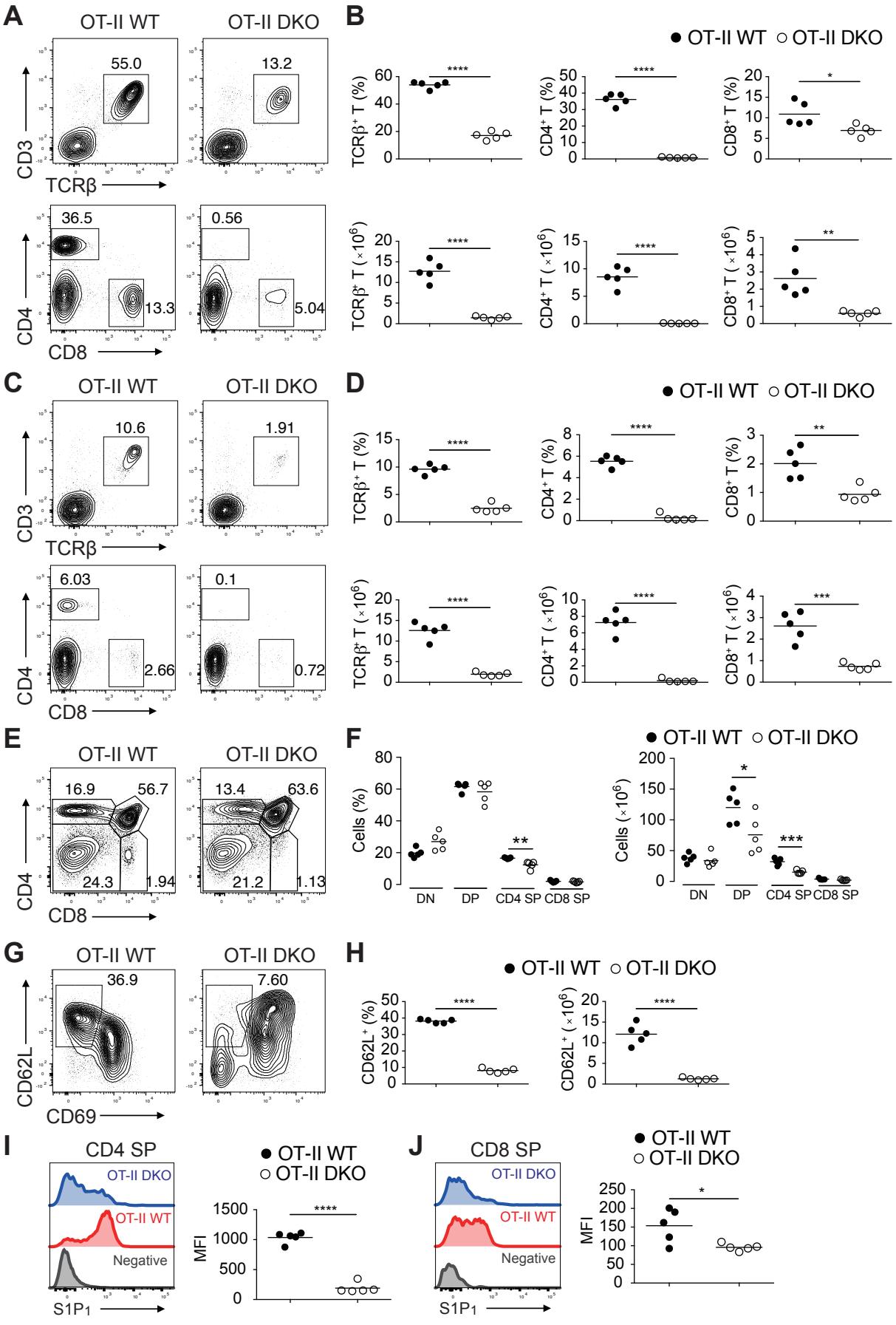
A
OT-II WT
OT-II DKO
55.0
13.2
CD3
TCRβ
36.5
0.56
13.3
5.04
CD4
CD8
B
● OT-II WT ○ OT-II DKO
TCRβ⁺ T (%)
CD4⁺ T (%)
CD8⁺ T (%)
TCRβ⁺ T (×10⁶)
CD4⁺ T (×10⁶)
CD8⁺ T (×10⁶)
****
*
**
C
10.6
1.91
6.03
0.1
2.66
0.72
D
***
E
16.9
56.7
24.3
1.94
13.4
63.6
21.2
1.13
F
Cells (%)
Cells (×10⁶)
DN
DP
CD4 SP
CD8 SP
G
36.9
7.60
CD62L
CD69
H
CD62L⁺ (%)
CD62L⁺ (×10⁶)
I
CD4 SP
OT-II DKO
OT-II WT
Negative
S1P1
MFI
J
CD8 SP

Fig. S6. The effect of *Gsk3*-deficiency on the development and egress of OT-II TCR transgenic thymocytes

(A-D) Flow cytometry analysis of $CD3^+TCR\beta^+$ (upper), $CD4^+$ and $CD8^+$ (lower) T cells in the lymph nodes (A) and spleen (C) of 4-6 week-old WT and DKO OT-II mice. (A and C) Representative FACS plots. (B and D) Summary of the percentage and number of $CD3^+TCR\beta^+$ (upper), $CD4^+$ and $CD8^+$ T cells (lower) (n≥3 per group). (E and F) Flow cytometry analysis of thymocyte development in mice in (A). (E) Representative FACS plots. (F) Summary of the percentage and number of DN, DP, CD4 and CD8 SP thymocytes. (G and H) Flow cytometry analysis of $CD62L^{hi}CD69^{lo}$ and $CD62L^{lo}CD69^{hi}$ cells among CD4 SP thymocytes in (E). (G) Representative FACS plots. (H) Summary of the percentage and number of $CD62L^{hi}CD69^{lo}$ cells among CD4 SP thymocytes. (I and J) $S1P_1$ expression on $CD62L^{hi}CD69^{lo}$ CD4 (I) and CD8 (J) SP thymocytes from WT and DKO OT-II mice was analyzed by flow cytometry. $CD62L^{lo}CD69^{hi}$ cells as a negative control (gray). Right panels, MFI of $S1P_1$ expression on $CD62L^{hi}CD69^{lo}$ CD4 (I) and CD8 (J) SP thymocytes of indicated genotypes. Each symbol represents an individual mouse. Small horizontal lines indicate the mean (± s.e.m.). *, $P < 0.1$; **, $P < 0.01$; ***, $P < 0.001$; ****, $P < 0.0001$. Data are representative of two independent experiments.

Fig. S7

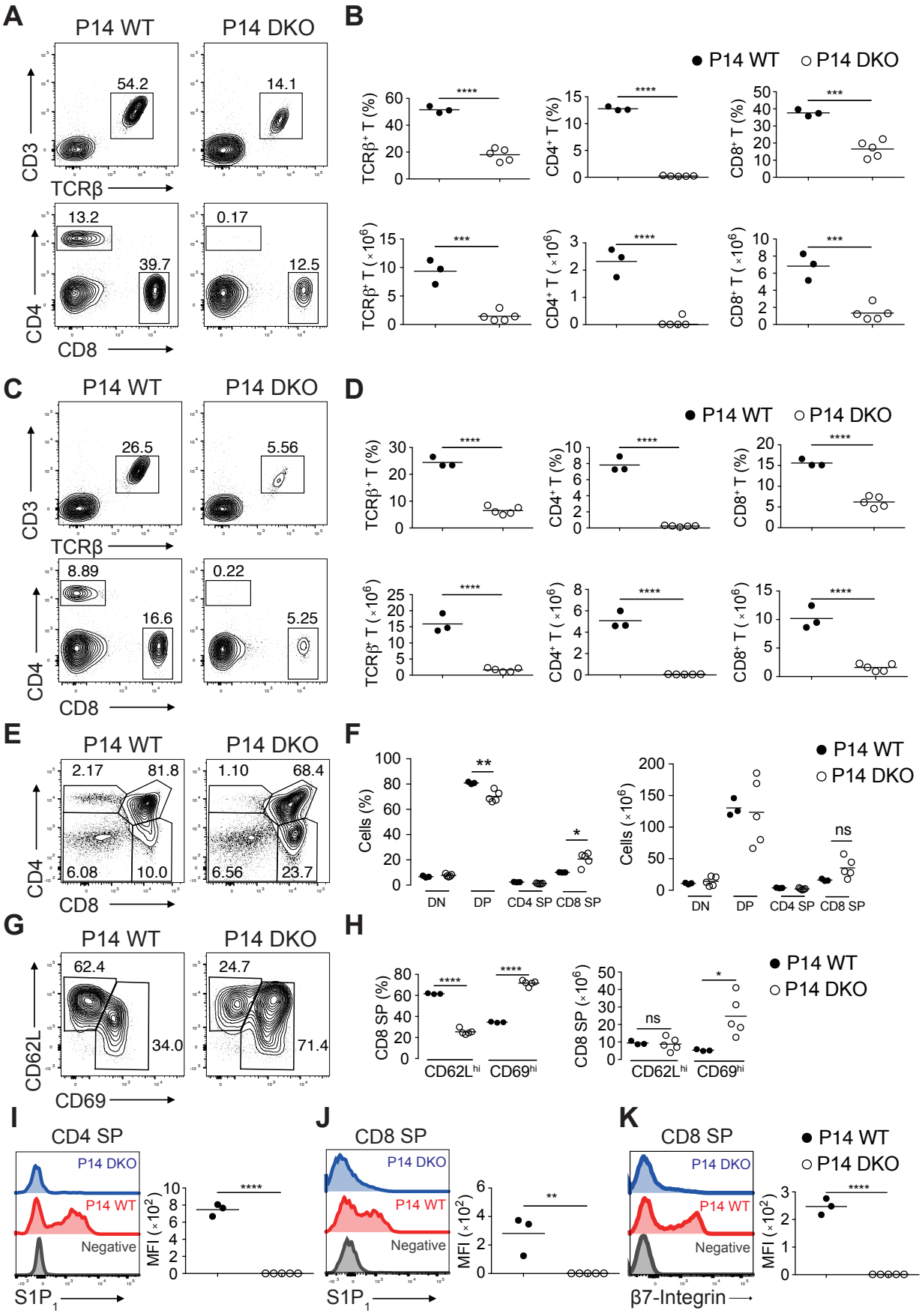
A
P14 WT
P14 DKO
54.2
14.1
CD3
TCRβ
13.2
39.7
0.17
12.5
CD4
CD8
B
P14 WT
P14 DKO
TCRβ+ T (%)
CD4+ T (%)
CD8+ T (%)
TCRβ+ T (×10^6)
CD4+ T (×10^6)
CD8+ T (×10^6)
C
P14 WT
P14 DKO
26.5
5.56
CD3
TCRβ
8.89
16.6
0.22
5.25
CD4
CD8
D
P14 WT
P14 DKO
TCRβ+ T (%)
CD4+ T (%)
CD8+ T (%)
TCRβ+ T (×10^6)
CD4+ T (×10^6)
CD8+ T (×10^6)
E
P14 WT
P14 DKO
2.17
81.8
1.10
68.4
CD4
CD8
6.08
10.0
6.56
23.7
F
P14 WT
P14 DKO
Cells (%)
Cells (×10^6)
DN
DP
CD4 SP
CD8 SP
ns
G
P14 WT
P14 DKO
62.4
24.7
CD62L
CD69
34.0
71.4
H
P14 WT
P14 DKO
CD8 SP (%)
CD8 SP (×10^6)
CD62L^hi
CD69^hi
ns
I
CD4 SP
P14 DKO
P14 WT
Negative
S1P1
MFI (×10^2)
J
CD8 SP
P14 DKO
P14 WT
Negative
S1P1
MFI (×10^2)
K
CD8 SP
P14 DKO
P14 WT
Negative
β7-Integrin
MFI (×10^2)
P14 WT
P14 DKO

Fig. S7. The effect of *Gsk3*-deficiency on the development and egress of P14 TCR transgenic thymocytes

(A-D) Flow cytometry analysis of $CD3^+TCR\beta^+$ (upper), $CD4^+$ and $CD8^+$ (lower) T cells in the lymph nodes (A) and spleen (D) of 4-6 week-old WT and DKO P14 mice. (A and C) Representative FACS plots. (B and D) Summary of the percentage and number of $CD3^+TCR\beta^+$ (upper), $CD4^+$ and $CD8^+$ T cells (lower) (n≥3 per group). (E and F) Flow cytometry analysis of thymocyte development in mice in (A). (E) Representative FACS plots. (F) Summary of the percentage and number of DN, DP, CD4 and CD8 SP thymocytes. (G and H) Flow cytometry analysis of $CD62L^{hi}CD69^{lo}$ and $CD62L^{lo}CD69^{hi}$ cells among CD8 SP thymocytes in (E). (G) Representative FACS plots. (H) Summary of the percentage and number of $CD62L^{hi}CD69^{lo}$ cells among CD8 SP thymocytes. (I and J) $S1P_1$ expression on $CD62L^{hi}CD69^{lo}$ CD4 (I) and CD8 (J) SP thymocytes from WT and DKO P14 mice was analyzed by flow cytometry. $CD62L^{lo}CD69^{hi}$ cells as a negative control (gray). Right panels, MFI of $S1P_1$ expression on $CD62L^{hi}CD69^{lo}$ CD4 (I) and CD8 (J) SP thymocytes of indicated genotypes. (K) β7-integrin expression on CD8 SP thymocytes in (G). Each symbol represents an individual mouse. Small horizontal lines indicate the mean (± s.e.m.). *, P <0.1; **, P <0.01; ***, P < 0.001; ****, P < 0.0001. Data are representative of two independent experiments.

Fig. S8

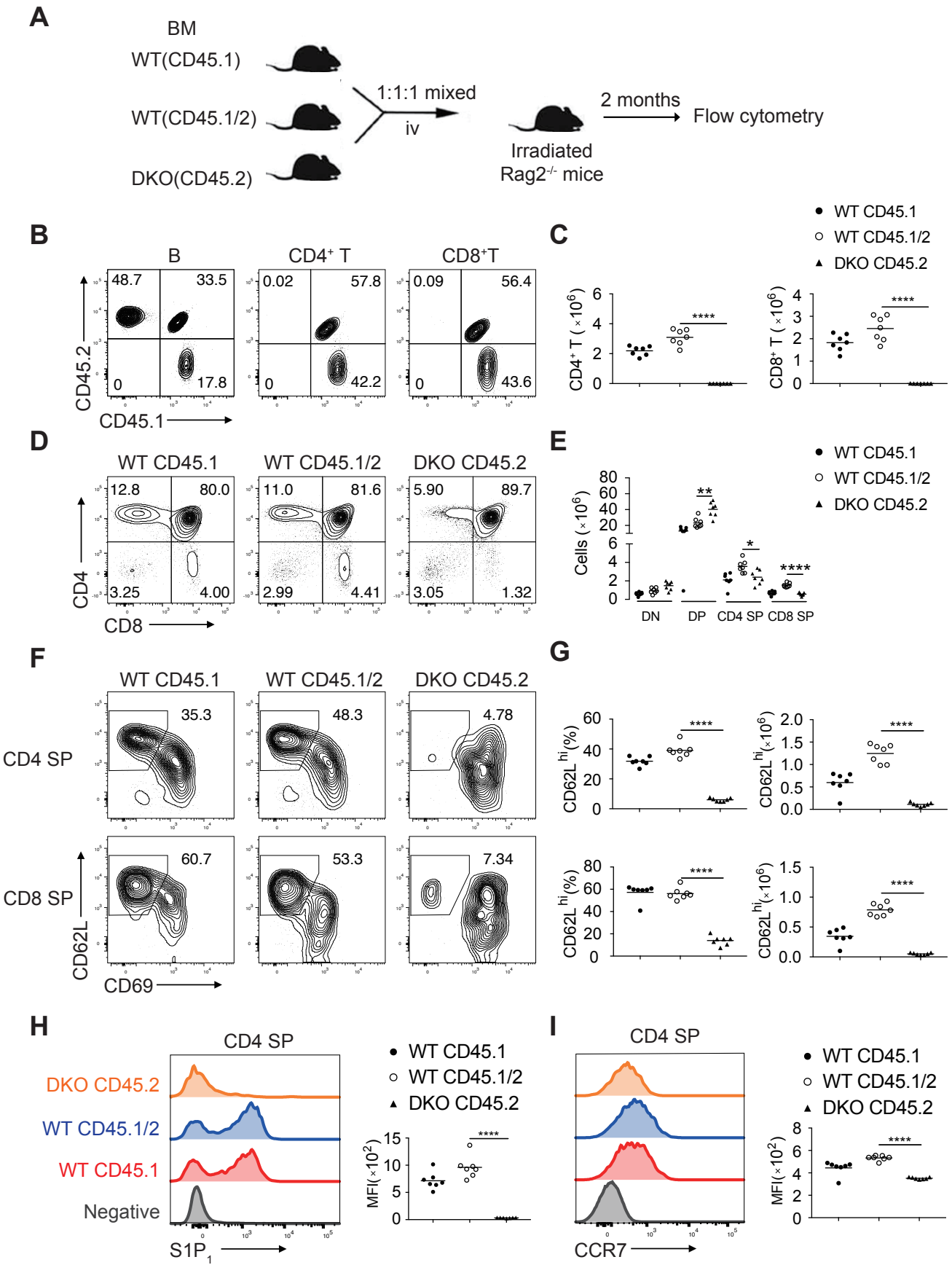
A
BM
WT(CD45.1)
WT(CD45.1/2)
DKO(CD45.2)
1:1:1 mixed
iv
Irradiated
Rag2-/- mice
2 months
Flow cytometry
B
B
CD4+ T
CD8+T
48.7
33.5
0
17.8
0.02
57.8
0
42.2
0.09
56.4
0
43.6
CD45.2
CD45.1
C
WT CD45.1
WT CD45.1/2
DKO CD45.2
CD4+ T (×10^6)
CD8+ T (×10^6)
****
D
WT CD45.1
WT CD45.1/2
DKO CD45.2
12.8
80.0
3.25
4.00
11.0
81.6
2.99
4.41
5.90
89.7
3.05
1.32
CD4
CD8
E
WT CD45.1
WT CD45.1/2
DKO CD45.2
Cells (×10^6)
DN
DP
CD4 SP
CD8 SP
F
WT CD45.1
WT CD45.1/2
DKO CD45.2
CD4 SP
CD8 SP
35.3
48.3
4.78
60.7
53.3
7.34
CD62L
CD69
G
CD62L hi (%)
CD62L hi (×10^6)
H
CD4 SP
DKO CD45.2
WT CD45.1/2
WT CD45.1
Negative
S1P1
MFI(×10^2)
I
CD4 SP
CCR7
MFI(×10^2)

Fig. S8. T cell-intrinsic role of GSK3 in thymocyte development and egress

(A) Experimental outline. Irradiated *Rag2*$^{-/-}$ mice were reconstituted with bone marrow cells from WT (CD45.1$^+$), WT (CD45.1$^+$/CD45.2$^+$) and DKO (CD45.2$^+$) mice in a 1:1:1 ratio and analyzed by flow cytometry 2 months after reconstitution. (B and C) Flow cytometry analysis of CD45.1$^+$ and CD45.2$^+$ cells among B, CD4$^+$ and CD8$^+$ T cells in the lymph nodes of mixed bone marrow chimeras in (A). (B) Representative FACS plots. (C) Summary of numbers of CD4$^+$ and CD8$^+$ T cells in (B) (n=7 per group). (D and E) Flow cytometry analysis of thymocyte development in mixed bone marrow chimeras in (A). (D) Representative FACS plots. (E) Summary of numbers of DN, DP, CD4 and CD8 SP thymocytes in (D) (n=7). (F and G) Flow cytometry analysis of CD62L^{hi}CD69^{lo} CD4 (upper) and CD8 (lower) SP thymocytes in mixed bone marrow chimeras in (A). (F) Representative FACS plots. (G) Summary of percentage and number of CD62L^{hi}CD69^{lo} cells in (F) (n=7). (H and I) Flow cytometry analysis of $S1P_1$ (H) and CCR7 (I) expression on CD62L^{hi}CD69^{lo} CD4 SP thymocytes in mixed bone marrow chimeras in (A). CD62L^{lo}CD69^{hi} cells as a negative control (gray). Right panels, MFI of $S1P_1$ (H) and CCR7 (I) expression on CD62L^{hi}CD69^{lo} CD4 SP thymocytes of indicated groups (n=7). Each symbol represents an individual mouse. Small horizontal lines indicate the mean (± s.e.m.). *, P <0.1; **, P <0.01; ****P < 0.0001. Data are representative of three independent experiments.

Fig. S9

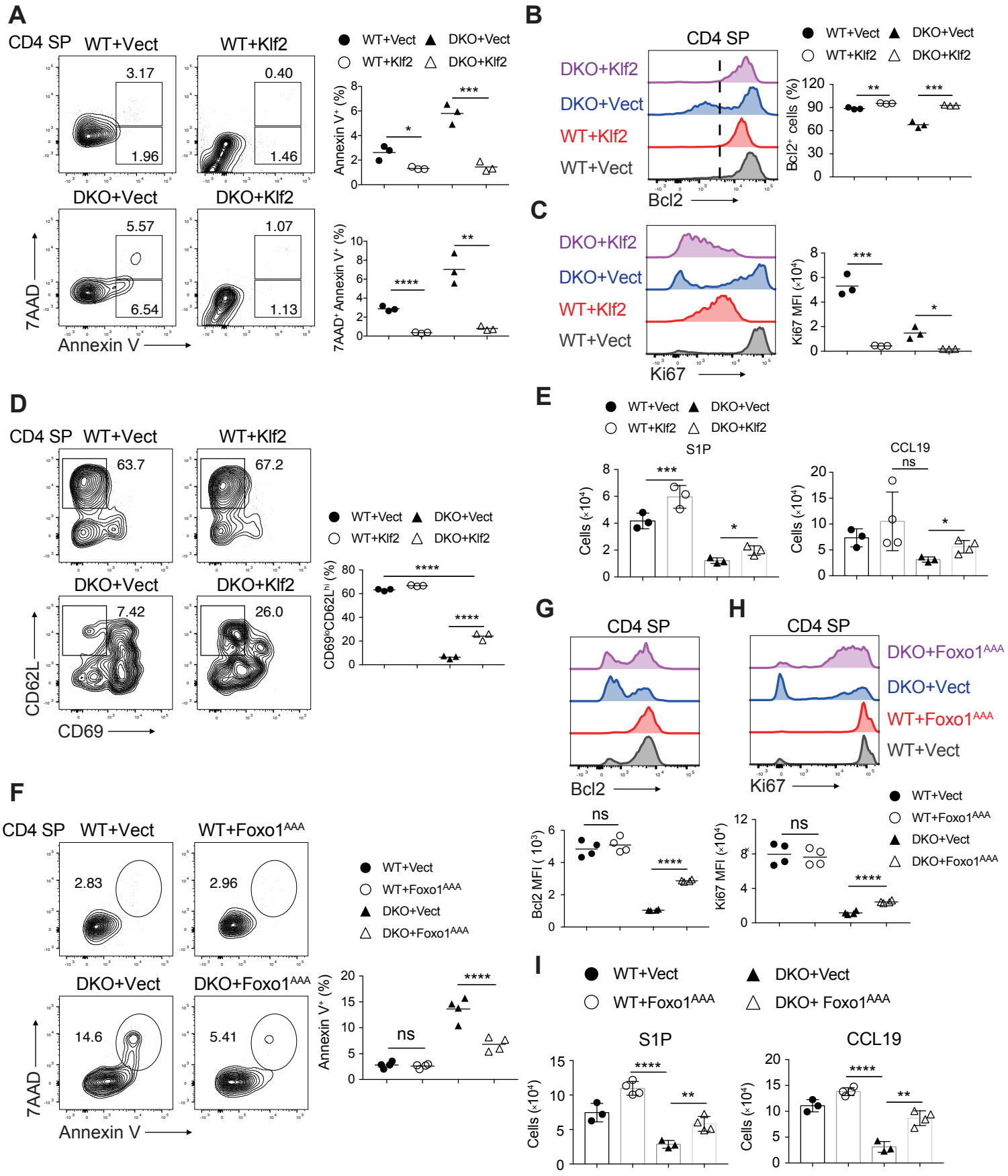
A
CD4 SP
WT+Vect
WT+Klf2
DKO+Vect
DKO+Klf2
3.17
1.96
0.40
1.46
5.57
6.54
1.07
1.13
7AAD
Annexin V
Annexin V⁺ (%)
7AAD⁺ Annexin V⁺ (%)
B
CD4 SP
Bcl2
Bcl2⁺ cells (%)
C
Ki67
Ki67 MFI (×10⁴)
D
63.7
67.2
7.42
26.0
CD62L
CD69
CD69ᵉCD62Lʰⁱ (%)
E
S1P
CCL19
Cells (×10⁴)
ns
F
WT+Foxo1AAA
DKO+Foxo1AAA
2.83
2.96
14.6
5.41
G
H
Bcl2 MFI (10³)
Ki67 MFI (×10⁴)
I

Fig. S9. Effects of Klf2 and constitutively active Foxo1 on the survival, proliferation and migration of *Gsk3*-deficient CD4 SP thymocytes.

(A-D) Flow cytometry analysis of apoptosis (Annexin V^+7AAD^+) (A), Bcl2 expression (B), proliferation ($Ki67^+$) (C), CD62L and CD69 expression (D) in DKO and WT CD4 SP thymocytes transduced with retroviruses encoding Klf2 or empty retroviruses (Vect). (E) Transwell migration assay of DKO and WT CD4 SP thymocytes transduced with retroviruses encoding Klf2 or empty retroviruses and stimulated with S1P (left) and CCL19 (right). (F-H) Flow cytometry analysis of apoptosis (Annexin V^+7AAD^+) (F), Bcl2 expression (G) and proliferation ($Ki67^+$) (H) of DKO and WT CD4 SP thymocytes transduced with retroviruses encoding Foxo1AAA or empty retroviruses (Vect). (I) Transwell migration assay of DKO and WT CD4 SP thymocytes transduced with retroviruses encoding Foxo1AAA or empty retroviruses and stimulated with S1P (left) and CCL19 (right). Each symbol represents an individual mouse. Small horizontal lines indicate the mean (± s.e.m.). *, P <0.1; **, P <0.01; ***, P <0.001; ****, P <0.0001. Data are representative of two independent experiments.

Fig. S10

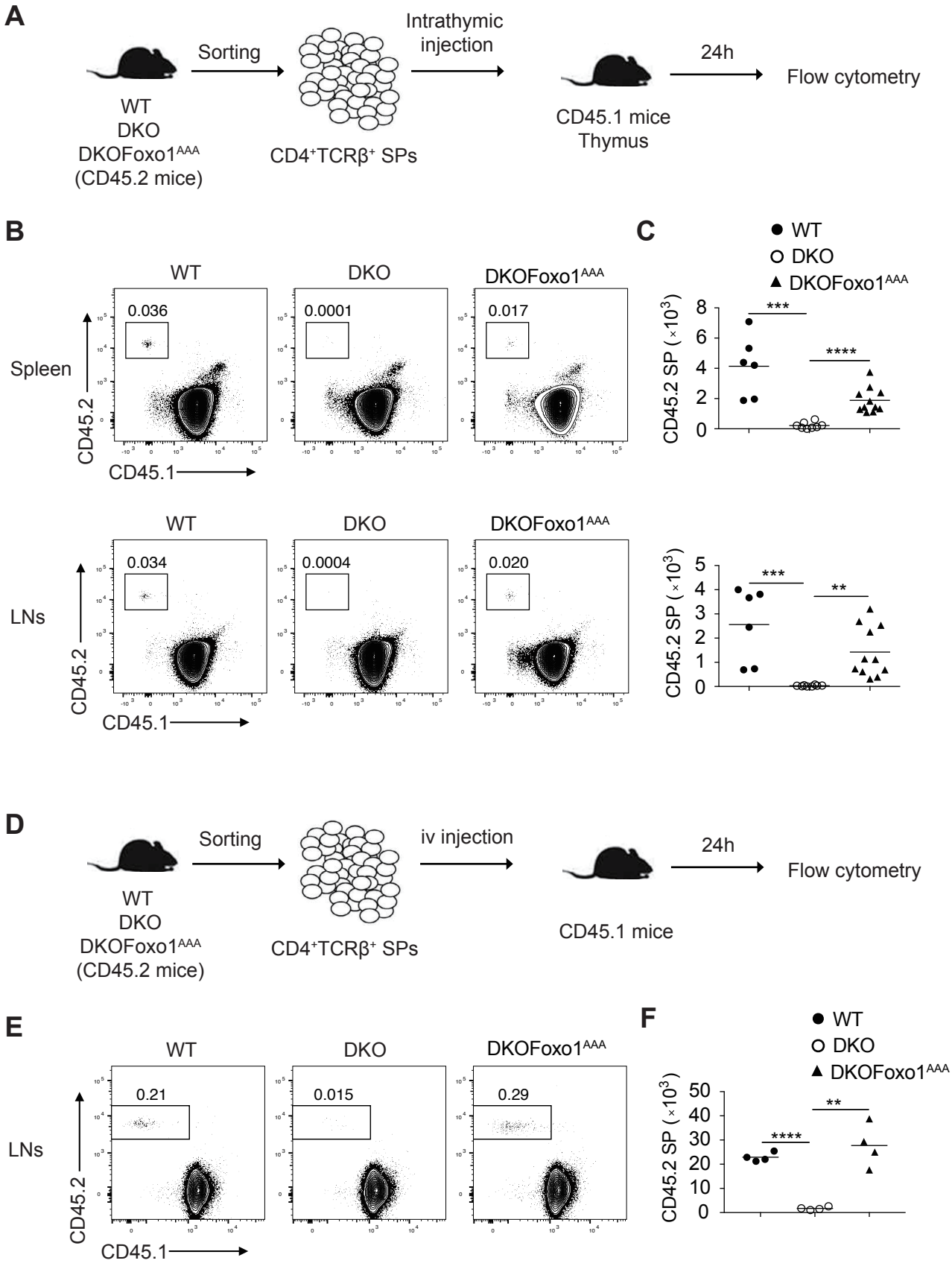
A
Sorting
Intrathymic injection
24h
Flow cytometry
WT
DKO
DKOFoxo1AAA
(CD45.2 mice)
CD4+TCRβ+ SPs
CD45.1 mice
Thymus
B
WT
DKO
DKOFoxo1AAA
Spleen
LNs
0.036
0.0001
0.017
0.034
0.0004
0.020
CD45.2
CD45.1
C
WT
DKO
DKOFoxo1AAA
CD45.2 SP (×10^3)
***
****
**
D
Sorting
iv injection
24h
Flow cytometry
WT
DKO
DKOFoxo1AAA
(CD45.2 mice)
CD4+TCRβ+ SPs
CD45.1 mice
E
LNs
0.21
0.015
0.29
CD45.2
CD45.1
F
WT
DKO
DKOFoxo1AAA
CD45.2 SP (×10^3)
****
**

Fig. S10. Constitutively actIve Foxo1 restores the egress and homing of *Gsk3*-deficient thymocytes

(A and D) Experimental outlines. $CD4^+TCR\beta^+$ SP thymocytes from WT, DKO and $DKOFoxo1^{AAA}$ mice (all $CD45.2^+$) were adoptively transferred into $CD45.1^+$ recipient mice by intrathymic (A) or intravenous (D) injection, followed by flow cytometry analysis at 24 hours after transfer. (B, C, E and F) Flow cytometry analysis of $CD45.2^+$ cells among $TCR\beta^+$ cells in the spleen and lymph nodes of recipient mice in (A and D). (B and E) Representative FACS plots. (C and F) Summary of number of $TCR\beta^+CD45.2^+$ cells in (B and E) ($n \geq 6$ per group). Each symbol represents an individual mouse. Small horizontal lines indicate the mean (± s.e.m.). **, $P < 0.01$; ***, $P < 0.001$; ****, $P < 0.0001$. Data are representative of two independent experiments.

Fig. S11

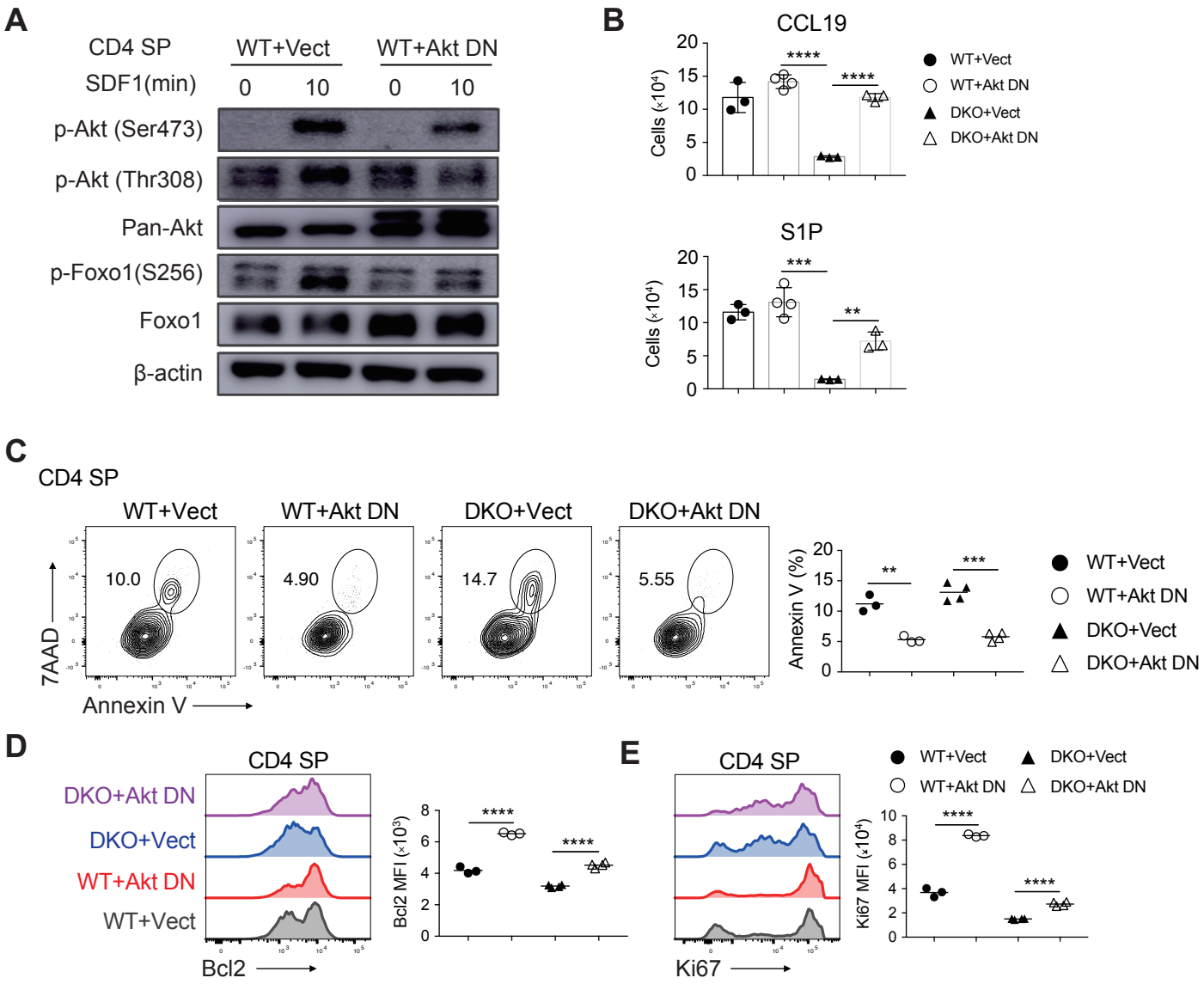
A
CD4 SP
WT+Vect
WT+Akt DN
SDF1(min)
0
10
0
10
p-Akt (Ser473)
p-Akt (Thr308)
Pan-Akt
p-Foxo1(S256)
Foxo1
β-actin
B
CCL19
Cells (×10⁴)
****
****
S1P
***
**
WT+Vect
WT+Akt DN
DKO+Vect
DKO+Akt DN
C
CD4 SP
WT+Vect
WT+Akt DN
DKO+Vect
DKO+Akt DN
10.0
4.90
14.7
5.55
7AAD
Annexin V
Annexin V (%)
**
***
D
CD4 SP
DKO+Akt DN
DKO+Vect
WT+Akt DN
WT+Vect
Bcl2
Bcl2 MFI (×10³)
****
****
E
CD4 SP
Ki67
Ki67 MFI (×10⁴)
****
****

Fig. S11. Effects of dominant negative Akt on the survival, proliferation and migration of *Gsk3*-deficient CD4 SP thymocytes.

(A) Immunoblot of p-Akt, pan-Akt, p-Foxo1, Foxo1 and β-actin in CD4 SP thymocytes from irradiated *Rag2*$^{-/-}$ mice reconstituted with WT bone marrow cells transduced with retroviruses encoding Akt-DN or empty retroviruses (Vect) and stimulated with SDF1 for 10 min. (B) Transwell migration assay of DKO and WT CD4 SP thymocytes transduced with retroviruses encoding Akt-DN or Vect and stimulated with CCL19 (upper) and S1P (lower). (C-E) Flow cytometry analysis of apoptosis (Annexin V^{+}7AAD^{+}) (C), Bcl2 expression (D) and proliferation (Ki67^{+}) (E) of DKO and WT CD4 SP thymocytes transduced with retroviruses encoding Akt-DN or empty retroviruses (Vect). Each symbol represents an individual mouse. Small horizontal lines indicate the mean (± s.e.m.). **, P <0.01; ***, P <0.001; ****, P < 0.0001. Data are representative of two independent experiments.

Fig. S12

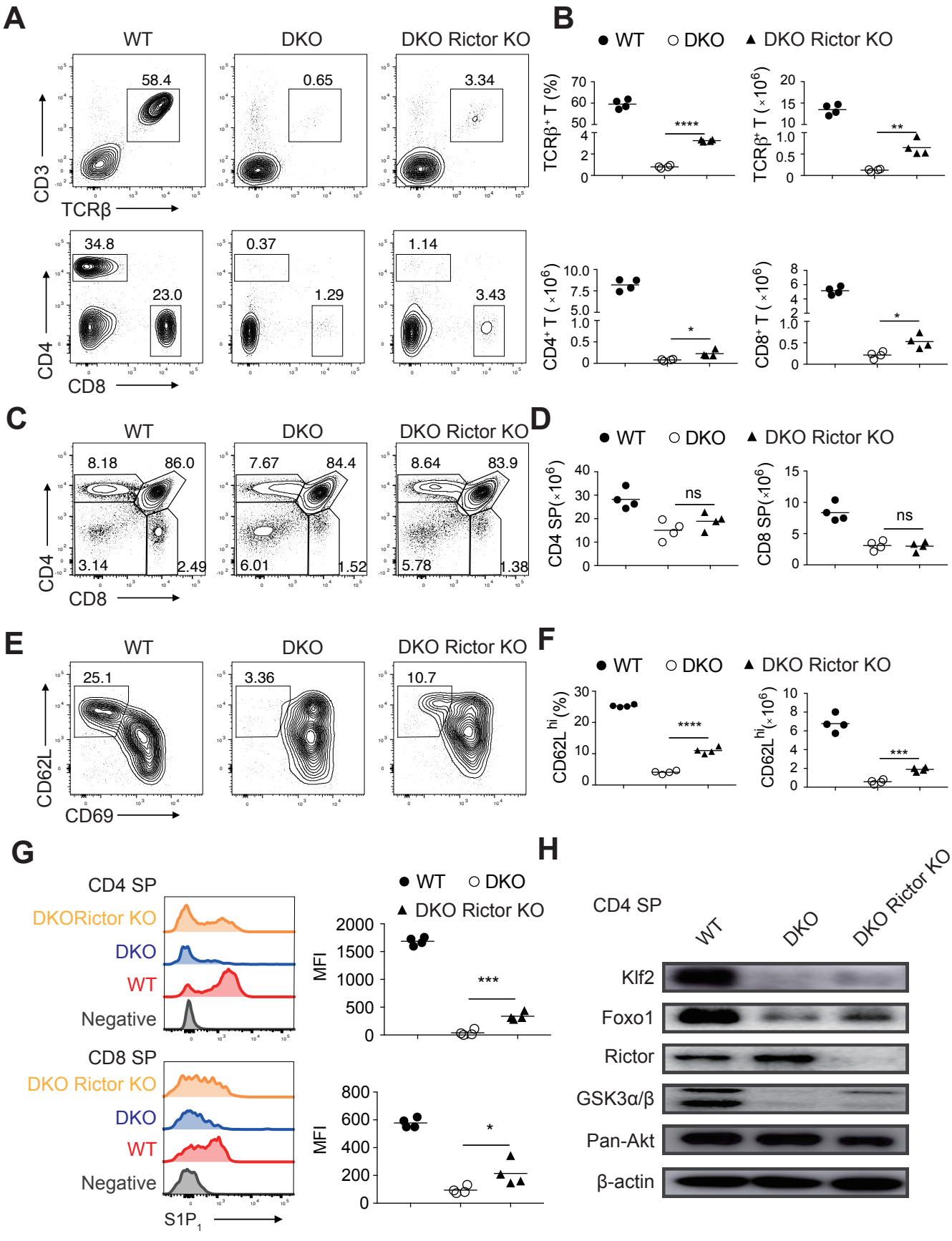
A
WT
DKO
DKO Rictor KO
58.4
0.65
3.34
CD3
TCRβ
34.8
23.0
0.37
1.29
1.14
3.43
CD4
CD8
B
WT
DKO
DKO Rictor KO
TCRβ+ T (%)
TCRβ+ T (×10^6)
CD4+ T (×10^6)
CD8+ T (×10^6)
****
**
*
C
8.18
86.0
3.14
2.49
7.67
84.4
6.01
1.52
8.64
83.9
5.78
1.38
D
CD4 SP(×10^6)
CD8 SP(×10^6)
ns
E
25.1
3.36
10.7
CD62L
CD69
F
CD62L hi (%)
CD62L hi (×10^6)
***
G
CD4 SP
DKORictor KO
DKO
WT
Negative
CD8 SP
DKO Rictor KO
S1P1
MFI
H
CD4 SP
Klf2
Foxo1
Rictor
GSK3α/β
Pan-Akt
β-actin

Fig. S12. Deletion of Rictor has a marginal effect on the egress of *Gsk3*-deficient thymocytes

(A) Flow cytometry analysis of $CD3^+TCR\beta^+$ (upper), $CD4^+$ and $CD8^+$ T (lower) cells in the lymph nodes of 4-6 week-old WT, DKO and *Gsk3a*$^{-/-}$*b*$^{-/-}$*Rictor*$^{-/-}$ (DKO Rictor KO) mice. (B) Summary of the percentage and number of $CD3^+TCR\beta^+$ (upper), $CD4^+$ and $CD8^+$ T cells (lower) in (A) (n≥4 per group). (C) Flow cytometry analysis of thymocyte development in mice in (A). (D) Summary of numbers of CD4 and CD8 SP thymocyte in (C). (E) Flow cytometry analysis of $CD62L^{hi}CD69^{lo}$ cells among CD4 SP thymocytes in mice in (A). (F) Summary of the percentage and number of $CD62L^{hi}CD69^{lo}$ cells among CD4 SP cells in (E). (G) $S1P_1$ expression on $CD62L^{hi}CD69^{lo}$ CD4 (upper) and CD8 (lower) SP thymocytes in mice in (A) was analyzed by flow cytometry. $CD62L^{lo}CD69^{hi}$ cells as a negative control (gray). Right panel, MFI of $S1P_1$ expression on $CD62L^{hi}CD69^{lo}$ CD4 SP thymocytes of indicated genotypes. (H) Immunoblot analysis of CD4 SP thymocytes of indicated genotypes. Each symbol represents an individual mouse. Small horizontal lines indicate the mean (± s.e.m.). *, P <0.1; **, P <0.01; ***, P < 0.001; ****, P < 0.0001. Data are representative of three independent experiments.

Fig. S13

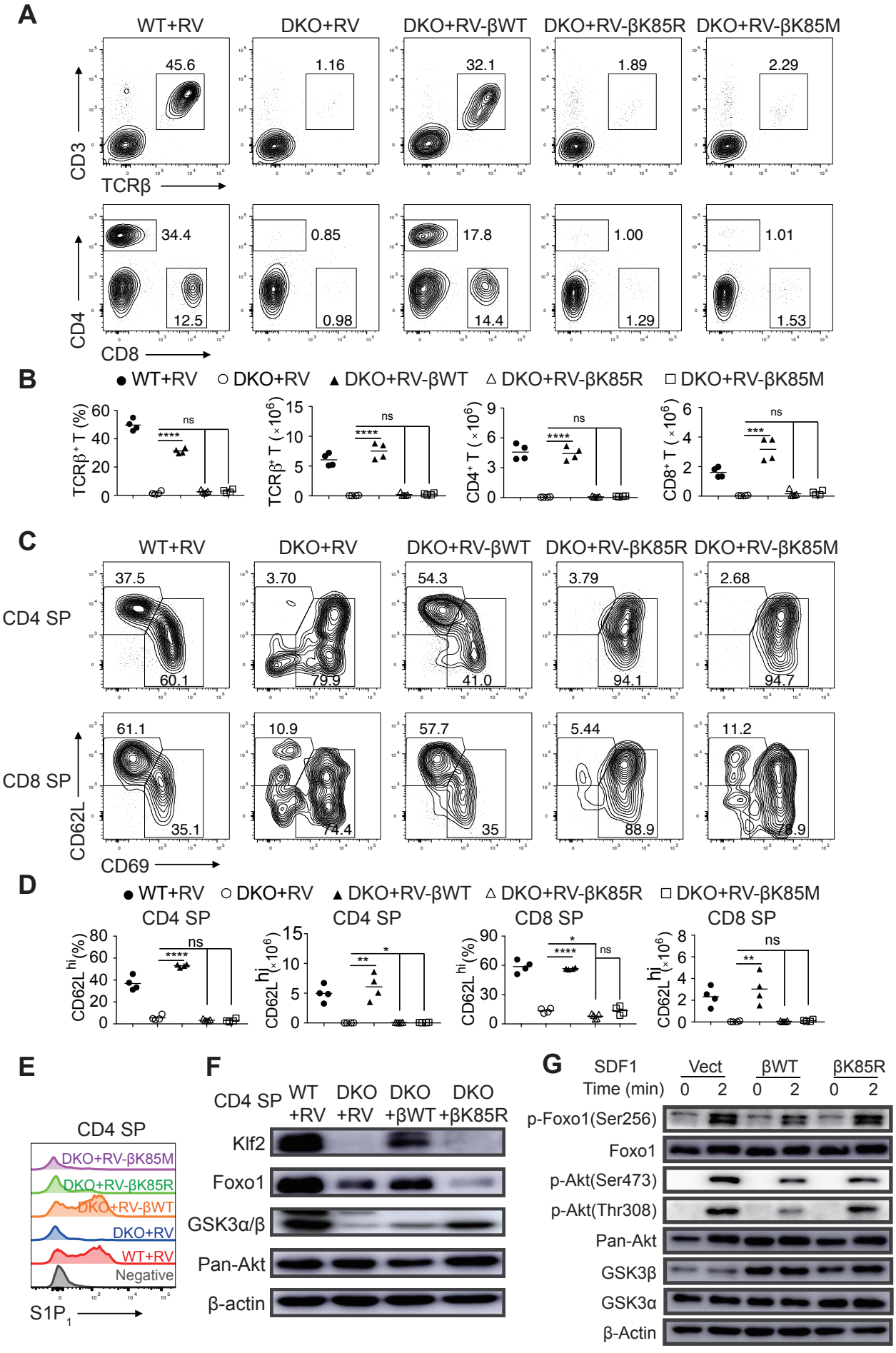
A
WT+RV
DKO+RV
DKO+RV-βWT
DKO+RV-βK85R
DKO+RV-βK85M
45.6
1.16
32.1
1.89
2.29
CD3
TCRβ
34.4
0.85
17.8
1.00
1.01
12.5
0.98
14.4
1.29
1.53
CD4
CD8
B
WT+RV
DKO+RV
DKO+RV-βWT
DKO+RV-βK85R
DKO+RV-βK85M
TCRβ+ T (%)
TCRβ+ T (×10^6)
CD4+ T (×10^6)
CD8+ T (×10^6)
ns
****
***
C
CD4 SP
CD8 SP
37.5
3.70
54.3
3.79
2.68
60.1
79.9
41.0
94.1
94.7
61.1
10.9
57.7
5.44
11.2
35.1
74.4
35
88.9
78.9
CD62L
CD69
D
CD4 SP
CD8 SP
CD62L hi (%)
CD62L hi (×10^6)
*
**
E
CD4 SP
DKO+RV-βK85M
DKO+RV-βK85R
DKO+RV-βWT
DKO+RV
WT+RV
Negative
S1P1
F
CD4 SP
WT +RV
DKO +RV
DKO +βWT
DKO +βK85R
Klf2
Foxo1
GSK3α/β
Pan-Akt
β-actin
G
SDF1
Time (min)
Vect
βWT
βK85R
0
2
p-Foxo1(Ser256)
Foxo1
p-Akt(Ser473)
p-Akt(Thr308)
Pan-Akt
GSK3β
GSK3α
β-Actin

Fig. S13. Kinase activity of GSK3 is essential for thymocyte egress

(A) Flow cytometry analysis of $CD3^+TCR\beta^+$ (upper), $CD4^+$ and $CD8^+$ (lower) T cells in the lymph nodes of recipient mice reconstituted with WT and DKO bone marrow cells transduced with empty retroviruses (RV) or retroviruses encoding wild type (RV-βWT) or kinase-dead GSK3β (RV-βK85R and βK85R). (B) Summary of the percentage and number of $CD3^+TCR\beta^+$ (upper), $CD4^+$ and $CD8^+$ T cells (lower) in (A) (n≥4 per group). (C) Flow cytometry analysis of $CD62L^{hi}CD69^{lo}$ and $CD62L^{lo}CD69^{hi}$ cells among on CD4 (upper) and CD8 (lower) SP thymocytes in the recipients in (A). (D) Summary of the percentage and number of $CD62L^{hi}CD69^{lo}$ cells among CD4 and CD8 SP thymocytes in (C). (E) $S1P_1$ expression on $CD62L^{hi}CD69^{lo}$ CD4 (upper) and CD8 (lower) SP thymocytes in mice in (A) was analyzed by flow cytometry. $CD62L^{lo}CD69^{hi}$ cells as a negative control (gray). (F) Immunoblot analysis of CD4 SP thymocytes of indicated groups. (G) Immunoblot analysis of CD4 SP thymocytes transduced with retroviruses encoding βWT or βK85R and stimulated with SDF1 for indicated amounts of time. Each symbol represents an individual mouse. Small horizontal lines indicate the mean (± s.e.m.). *, P <0.1; **, P <0.01; ***, P < 0.001; ****, P < 0.0001. Data are representative of three independent experiments.

Fig. S14

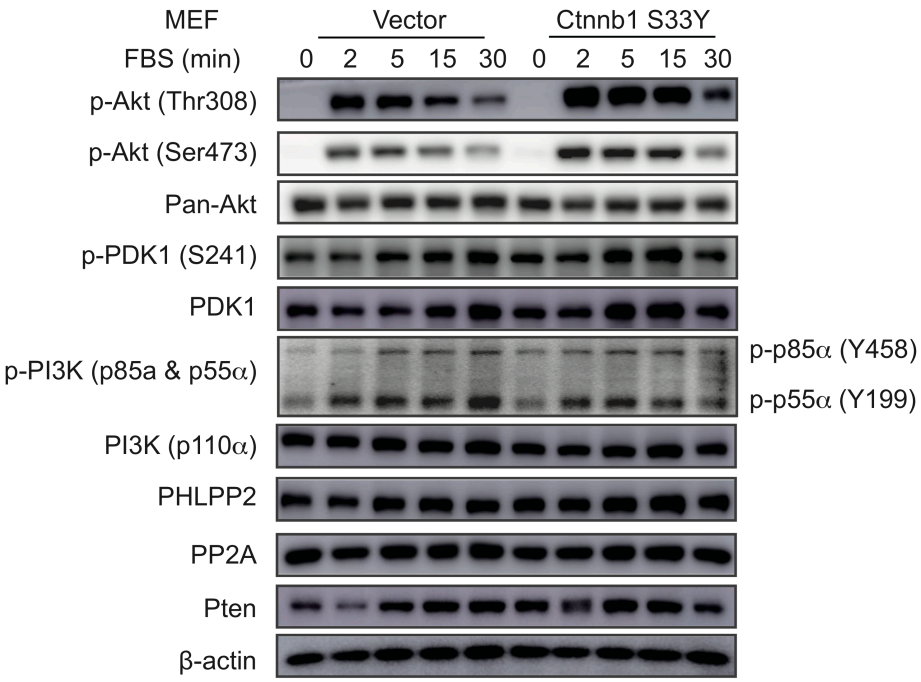
MEF
Vector
Ctnnb1 S33Y
FBS (min)
0 2 5 15 30 0 2 5 15 30
p-Akt (Thr308)
p-Akt (Ser473)
Pan-Akt
p-PDK1 (S241)
PDK1
p-PI3K (p85a & p55α)
p-p85α (Y458)
p-p55α (Y199)
PI3K (p110α)
PHLPP2
PP2A
Pten
β-actin

Fig. S14. Stabilized β-catenin does not affect PI3K and PDK1 activation

MEFs were transduced with lentiviruses encoding β-catenin S33Y (Ctnnb1 S33Y) or vector, serum starved for 16 hours, and re-stimulated with 0.5% FBS for indicated amounts of time. Total cell lysates were analyzed by immunoblotting with indicated antibodies. Data are representative of two independent experiments.

Fig. S15

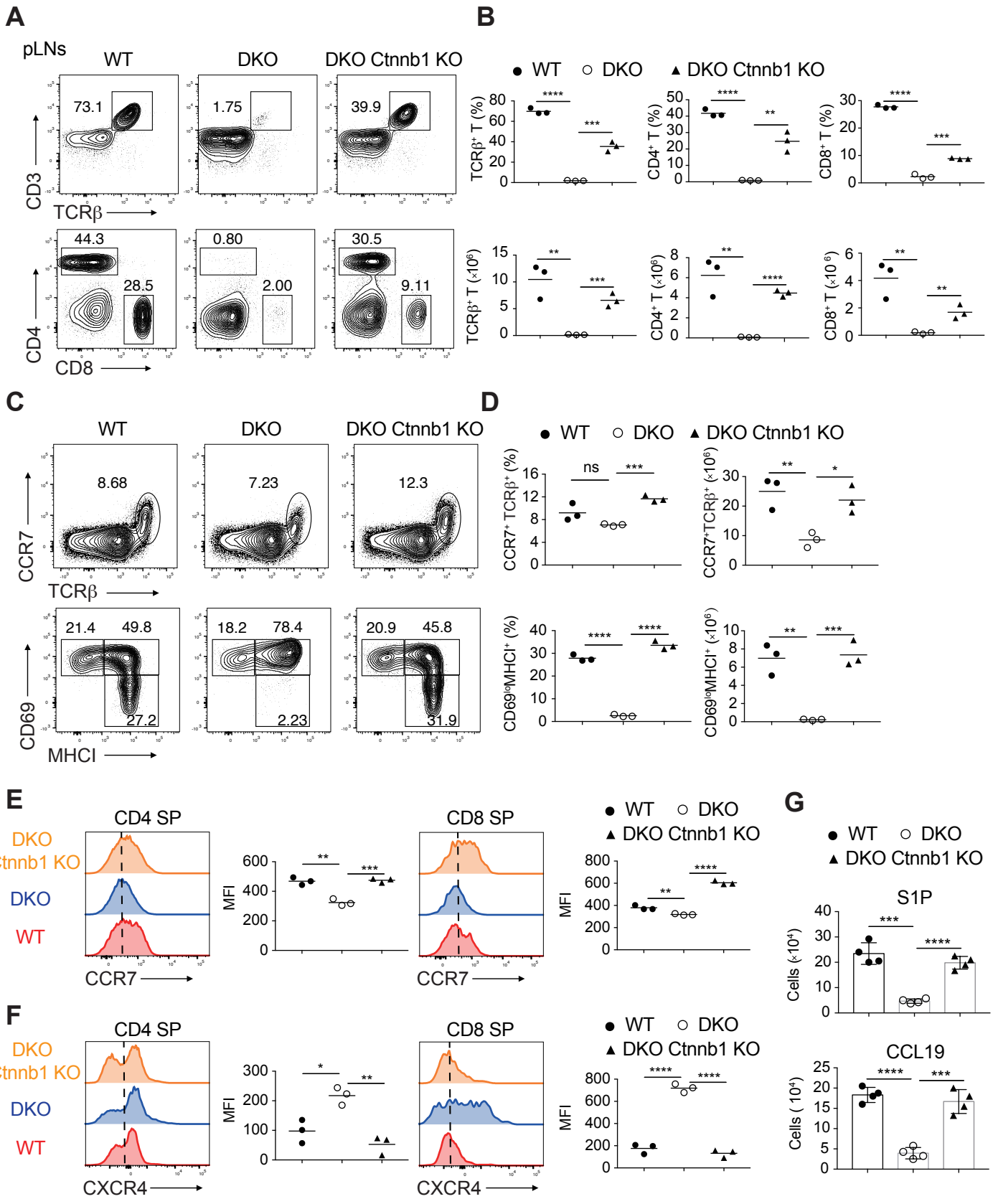
A
pLNs
WT
DKO
DKO Ctnnb1 KO
73.1
1.75
39.9
CD3
TCRβ
44.3
28.5
0.80
2.00
30.5
9.11
CD4
CD8
B
WT
DKO
DKO Ctnnb1 KO
TCRβ+ T (%)
CD4+ T (%)
CD8+ T (%)
TCRβ+ T (×10^6)
CD4+ T (×10^6)
CD8+ T (×10^6)
C
8.68
7.23
12.3
CCR7
TCRβ
21.4
49.8
27.2
18.2
78.4
2.23
20.9
45.8
31.9
CD69
MHCI
D
ns
CCR7+ TCRβ+ (%)
CCR7+TCRβ+ (×10^6)
CD69loMHCI+ (%)
CD69loMHCI+ (×10^6)
E
CD4 SP
CD8 SP
DKO Ctnnb1 KO
DKO
WT
CCR7
MFI
F
CXCR4
G
S1P
CCL19
Cells (×10^4)
Cells (10^4)

Fig. S15. *Ctnnb1* deletion restores CCR7 and CXCR4 expression and migration of mature *Gsk3*-deficient thymocytes

(A) Flow cytometry analysis of $CD3^+TCR\beta^+$ (upper), $CD4^+$ and $CD8^+$ T (lower) cells in the lymph nodes of 4-6 week-old WT, DKO and *Gsk3a*$^{-/-}$*b*$^{-/-}$*Ctnnb1*$^{-/-}$ (DKO Ctnnb1 KO) mice. (B) Summary of the percentage (upper) and number (lower) of $CD3^+TCR\beta^+$, $CD4^+$ and $CD8^+$ T cells in (A) (n=3 per group). (C) Flow cytometry analysis of CCR7 and TCRβ expression by total thymocytes from WT, DKO and DKO Ctnnb1 KO mice (upper). Post-positive selection thymocytes ($CCR7^+TCR\beta^+$) were subsetted into three subpopulations (SM, M1 and M2) based on CD69 and MHC I expression (lower). (D) Summary of the percentage and number of $CCR7^+TCR\beta^+$ (upper) and $CD69^{lo}MHCI^+$ (lower) cells among CD4 SP cells in (C). (E and F) CCR7 (E) and CXCR4 (F) expression on $CD62L^{hi}CD69^{lo}$ CD4 (left) and CD8 (right) SP thymocytes in mice in (A) was analyzed by flow cytometry. Right panel, MFI of CCR7 and CXCR4 expression on $CD62L^{hi}CD69^{lo}$ CD4 SP thymocytes of indicated genotypes. (G) Transwell migration assay of WT, DKO and DKO Ctnnb1 KO CD4 SP thymocytes in response to S1P (upper) and CCL19 (lower). Each symbol represents an individual mouse. Small horizontal lines indicate the mean (± s.e.m.). *, P <0.1; **, P <0.01; ***, P < 0.001; ****, P < 0.0001. Data are representative of three independent experiments.